European Journal of Human Genetics (2009) 17, 1024 – 1033

www.nature.com/ejhg

ARTICLE

Characterization of two ectrodactyly-associated translocation breakpoints separated by 2.5 Mb on chromosome 2q14.1–q14.2

Dezső David*,[1], Bárbara Marques[1], Cristina Ferreira[1], Paula Vieira[1], Alfredo Corona-Rivera[2], José Carlos Ferreira[3] and Hans van Bokhoven[4]

[1]*Department of Genetics, National Institute of Health Dr Ricardo Jorge, Lisboa, Portugal;* [2]*Department of Molecular Biology and Genomics, University of Guadalajara, Guadalajara, México;* [3]*Obstetrics Department, Prenatal Diagnosis Centre, Garcia de Orta Hospital, Almada, Portugal;* [4]*Department of Human Genetics, Nijmegen Centre for Molecular Life Sciences, Radboud University, Nijmegen Medical Centre, Nijmegen, The Netherlands*

Split hand-split foot malformation or ectrodactyly is a heterogeneous congenital defect of digit formation. The aim of this study is the mapping of the breakpoints and a detailed molecular characterization of the candidate genes for an isolated and syndromic form of ectrodactyly, both associated with *de novo* apparently balanced chromosome translocations involving the same chromosome 2 band, [t(2;11)(q14.2;q14.2)] and [t(2;4)(q14.1;q35)], respectively. Breakpoints were mapped by fluorescence *in situ* hybridization using bacterial artificial chromosome clones. Where possible, these breakpoints were further delimited. Candidate genes were screened for pathogenic mutations and the expression levels of two of them analysed. The isolated bilateral split foot malformation-associated chromosome 2 breakpoint was localized at 120.9 Mb, between the two main candidate genes, encoding GLI-Kruppel family member GLI2 and inhibin-βB. The second breakpoint associated with holoprosencephaly, hypertelorism and ectrodactyly syndrome was mapped 2.5 Mb proximal at 118.4 Mb and the candidate genes identified from this region were the insulin-induced protein 2 and the homeobox protein engrailed-1. No clear pathogenic mutations were identified in any of these genes. The breakpoint between *INHBB* and *GLI2* coincides with a previously identified translocation breakpoint associated with ectrodactyly. We propose a mechanism by which translocations in the 2q14.1–q14.2 region disrupt the specific arrangement of long-range regulatory elements that control the tight quantitative spatiotemporal expression of one or more genes from the breakpoint region.

European Journal of Human Genetics (2009) **17,** 1024–1033; doi:10.1038/ejhg.2009.2; published online 18 February 2009

Keywords: ectrodactyly-associated chromosomal translocations; chromosome 2q14.1–q14.2; GLI2; INHBB; INSIG2

Introduction

Split hand-split foot malformation (SHFM; OMIM 225300) or ectrodactyly is a congenital defect of digit formation characterized by aplasia of the central digits with fusion of the remaining digits. Most cases are isolated with autosomal-dominant inheritance and incomplete penetrance, but some pedigrees with autosomal-recessive or even X-linked forms have also been reported (reviewed by

***Correspondence: Dr D David, Departamento de Genética, Instituto Nacional de Saúde Dr Ricardo Jorge, Av. Padre Cruz, 1649-016 Lisboa, Portugal. Tel: +351 217519322; Fax: +351 217526410;**
E-mail: dezso.david@insa.min-saude.pt
Received 27 March 2008; revised 22 December 2008; accepted 8 January 2009; published online 18 February 2009

Duijf *et al*[1]). Ectrodactyly also occurs in several syndromes and can be found associated with a variety of other developmental anomalies.

To date, at least six SHFM *loci* have been implicated in the pathogenesis of syndromic or isolated ectrodactylies, but up to now only two causative genes have been identified. Mutations in *TP63*, a paralogue of the tumour-suppressor gene *TP53*, are responsible for ectrodactyly-ectodermal dysplasia-cleft lip/palate syndrome (EEC; OMIM 604292) and related conditions, such as acro-dermato-ungual-lacrimal-tooth syndrome (ADULT; OMIM 103285), limb-mammary syndrome (LMS; OMIM 603543), Rapp-Hodgkin syndrome (RHS; OMIM 129400), and Ankyloblepharon-Ectodermal Dysplasia Clefting or Hay-Wells syndrome (AEC; OMIM 106260). In addition, *TP63* mutations account for approximately 10% of non-syndromic or isolated forms of ectrodactyly, denoted by SHFM4 (reviewed by van Bokhoven and Brunner[2]). Recently, Kjaer *et al*[3] reported that homozygous mutations in the cadherin-3 gene (*CDH3*) cause ectodermal dysplasia, ectrodactyly and macular dystrophy syndrome (EEM; OMIM 225280).

Additional SHFM *loci* have been mapped: SHFM1 to chromosome 7q21.3–q22.1 region (Bernardini *et al*[4] and references therein); SHFM3 to chromosome 10q24, associated with a large ~0.5 Mb tandem duplication including the ladybird homeobox 1 (*LBX1*), the *β*-transducin repeat containing (β*TRC*), the Pol lambda (*POLL*) genes and a portion of the *FBXW4* or *DACTYLIN* gene;[5] and several *loci* in the 2q24–q31 region, including SHFM5.[1,6] Recently, a new *locus*, SHFM6 in 8q21.11–q22.3, was suggested on the basis of a genome-wide linkage analysis in a single family.[7]

Ectrodactyly has been repeatedly reported in association with a variety of other developmental anomalies. As an example, a holoprosencephaly, hypertelorism and ectrodactyly syndrome (HHES), considered as an independent clinical entity, was reported to be associated with an apparently balanced *de novo* translocation [t(2;4)(q14.2;q35)] in a Mexican patient.[8] In addition to this case, an association of ectrodactyly with holoprosencephaly has been reported in six additional probands (reviewed by König *et al*[9]).

Recently, two novel susceptibility *loci* for split-hand/foot malformation with long-bone deficiency (SHFLD) were identified on chromosomes 1q42.2–q43 and 6q14.1.[10] Interestingly, a translocation involving chromosome 2q14.2 was recently reported in another patient with SHFLD, which led to the postulation of a new SHFM locus on 2q14.2.[11]

In this study, we characterize the breakpoints of a *de novo* apparently balanced chromosomal translocation [t(2;11)(q14.2;q14.2)] associated with bilateral split foot malformation (SFM) identified in a fetus during ultrasound prenatal screening. Furthermore, we also mapped the chromosome 2 breakpoint identified in the previously reported Mexican proband with HHES.

Materials and methods

Probands, patients and controls

The probands are described in the Results section. A group of 35 unrelated patients with either typical, atypical, isolated or syndromic forms of SHFM and a control group of about 100 unrelated individuals were used for mutation screening of the candidate genes.

Lymphoblastoid cell line, bacterial artificial chromosome clones and isolation of DNAs

Following informed consent from the parents, fetal blood sample was obtained after voluntary termination of pregnancy from the umbilical vein and a lymphoblastoid cell line (LCL) was established. Bacterial artificial chromosome (BAC) clones were obtained from the Sanger Institute (Hinxton, Cambridge, UK) and the BACPAC Resources Center at Children's Hospital Oakland Research Institute (Oakland, CA, USA).

Genomic DNA was prepared from peripheral blood lymphocytes and LCLs by standard molecular techniques. LCL or DNA samples were unavailable from the Mexican proband with HHES. BAC DNA was extracted by the alkaline lysis method performed according to the protocol from the Hubbard Center for Genome Studies (http://hcgs.unh.edu/protocol/BAC/).

Chromosome analysis, chromosome comparative genomic hybridization and *in situ* hybridization

Metaphase and prometaphase chromosome preparations were obtained from LCLs and phytohemagglutinin-stimulated lymphocytes by standard cytogenetic techniques. Cytogenetic analysis was performed on conventional Trypsin-Leishman G-banded metaphases. Only three chromosome slides were available from the proband with HHES.

For conventional chromosome comparative genomic hybridisation (CGH), SpectrumRed direct-labelled genomic DNA (Vysis Inc., Downers Grove, IL, USA) was used as control, whereas the patients' DNA was biotin labelled. Hybridization, post-hybridization washes and analysis using the ISIS-CGH software from MetaSystems (Altlusshein, Germany) were essentially performed as described earlier (Van Roy *et al*[12]).

BAC DNAs, purified long-range PCR fragments amplified using the Expand Long Template PCR System (Roche Diagnostics, Mannheim, Germany), and reamplified PCR fragments using the GenomiPhi DNA amplification kit (GE Healthcare Life Sciences, Uppsala, Sweden) were used as FISH probes for mapping the translocation breakpoints. Amplifications were performed in a total volume of 50 μl according to the manufacturer's instructions. Labelling of

these probes and FISH analysis were performed as described earlier.[13]

Mutation screening of the candidate genes

Mutation screening of the candidate genes, inhibin-βB gene (*INHBB*), GLI-Kruppel family member *GLI2*, insulin-induced protein 2 (*INSIG2*), engrailed homeobox 1 (*EN1*) and the predicted gene XR_017842, in the unrelated patient group with different forms of syndromic and nonsyndromic SHFM, was performed by direct sequencing using the Big Dye Terminator cycle sequencing kit (Applied Biosystems). Products were separated on the ABI PRISM 3130XL Genetic Analyzer according to the manufacturer's instructions.

The sequence of the oligonucleotide primers and PCR conditions used for the amplification of the entire coding regions, exon–intron junctions and part of the 5′ and 3′ untranslated regions (UTR) of the candidate genes are available on request.

Screening of the control group and additional family members for the presence of the identified potential pathogenic mutations was carried out by single-stranded conformation polymorphism analysis or restriction enzyme cleavage and direct sequencing, performed as described earlier.[13,14] The screening conditions are also available on request.

Quantitative reverse transcriptase-PCR

SYBR Green-based quantitative reverse transcriptase (QRT)-PCR analysis was performed on a 7500 Fast Real-Time PCR System by using Power SYBR Green PCR Master Mix (Applied Biosystems, Foster City, CA, USA) according to the manufacturer's instructions. Primer pairs were developed for *INHBB* exon 2, *GLI2* exons 3-4, exon 7 and exons 8–9. The qPCR primer pairs were validated as described earlier.[15] The sequences of the primers are available on request. β-glucuronidase was used as a reference gene.[15]

Quantitative PCR quantifications were performed in duplicate on an equivalent of 400 pg/µl of total RNA input in the first strand synthesis, and included a reverse transcriptase control. The melt curves of all PCR products showed a single PCR product.

Results

Probands and cytogenetic analysis

The first proband, a fetus, was identified on the second trimester routine ultrasound anatomy scan as having a limb malformation, namely bilateral SFM or ectrodactyly of the lower limbs (Figure 1a). This was the first pregnancy of a nonconsanguineous couple of Portuguese origin. Both parents were phenotypically normal and there was no report of any limb abnormality in their families. A follow-up ultrasound examination suggested mild brain ventriculomegaly (atria width 10–11 mm).

Cytogenetic analysis performed from cultured amniotic fluid cells of the fetus revealed a *de novo* apparently balanced reciprocal chromosomal translocation [t(2;11)(q14.2;q14.2)] (Figure 1b). Both parents were cytogenetically normal. Larger genomic imbalances were ruled out on the basis of chromosome CGH (data not shown), and the reciprocity of the translocation was confirmed by FISH analysis (Figure 1c).

Given the uncertainty of the prognosis in this type of situations, termination of pregnancy was requested and performed at ~23 to 24 weeks of pregnancy. Morphopathological evaluation confirmed the SFM but failed to confirm clinically significant ventriculomegaly. No other anomaly of the brain, limbs or other organs was reported.

The clinical features of the second proband with HHES associated with the *de novo* translocation [t(2;4)(q14.2;q35)] (Figure 2a) were described earlier.[8]

Comparative mapping of the two chromosomes 2 breakpoints

BAC clones were selected on the basis of the cytogenetically established chromosome breakpoint regions (Figure 2a and b) using the ensemble database. These were hybridized against metaphase chromosome spreads of the two probands. The chromosome 2 breakpoint associated with isolated SFM was found to be within BAC clone RP13-1012F16 (Figures 1d and 2b) in distal 2q14.2. Fine mapping of this breakpoint was performed within the sequence AC114732 (BAC clone RP13-1012F16) using long-range PCR-generated fragments as FISH probes. The smallest breakpoint-spanning FISH fragment identified was 6.2 kb (between nucleotide positions 73 359 to 79 576 of AC114732). The approximate localization of the breakpoint is at position 120 922 kb of chromosome 2.

The chromosome 2 breakpoint associated with HHES was found upstream, within the BAC clone RP11-28H22 (localized at 118 292–118 404 kb) (Figures 1f and 2a), in distal q14.1. Owing to the lack of additional samples from this proband, further refinement of this candidate *locus* is impossible. The two breakpoints are approximately 2.5 Mb apart (Figure 3).

Identification of candidate genes from the chromosome 2 breakpoint regions

The chromosome 2 breakpoint associated with isolated SFM was localized about 100 kb distal to the inhibin-βB gene (*INHBB*) and 350 kb proximal to the GLI-Kruppel zinc-finger transcription factors family member GLI2 gene (*GLI2*). Between these two genes, there is an additional predicted gene XR_017842 that codes for the hypothetical protein FLJ14816. The breakpoint is about 15 kb proximal to this hypothetical gene (Figure 4).

Our data indicate that the chromosome 2 breakpoint associated with HHES is within the genomic region (Figure 3) bounded proximally by the DEAD box protein

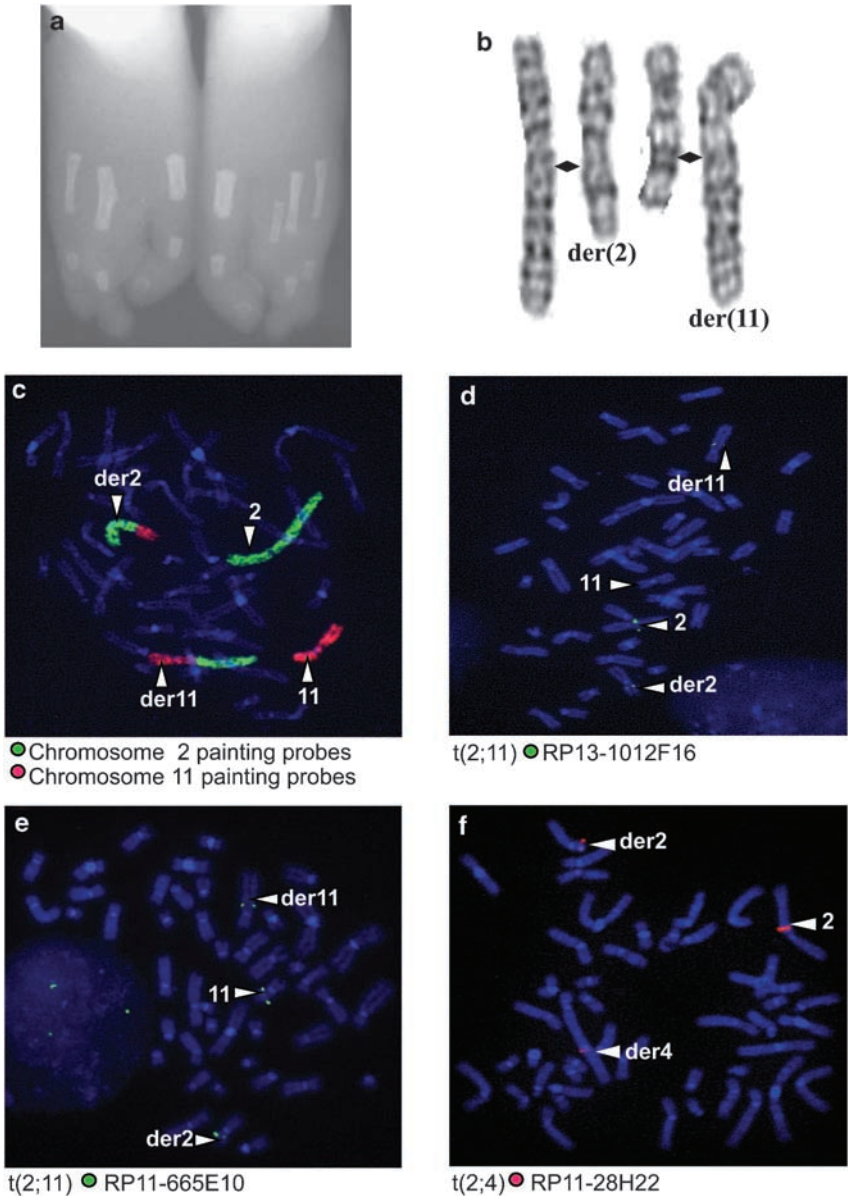

Figure 1 Clinical phenotype, partial karyotype and FISH mapping. (**a**) X-ray showing bilateral SFM. (**b**) The wild-type and derivative (der) chromosomes of the *de novo* translocation [t(2;11)(q14.2;q14.2)] (◆ indicate chromosome breakpoints). (**c**) Chromosome painting with chromosome 2 (green) and 11 (red) specific library probes. (**d**) FISH mapping of the chromosome 2 breakpoint of the t(2;11) with clone RP13-1012F16. Signals (green) were detected on the normal chromosome 2 and both derivative chromosomes. (**e**) FISH mapping of the chromosome 11 breakpoint with clones RP11-665E10. Signals (green) were detected on normal chromosome 11, der(11) and der(2). (**f**) FISH mapping of the chromosome 2 breakpoint of the t(2;4) with clone RP11-28H22. Signals (red) were detected on normal chromosome 2 and both derivative chromosomes.

18 gene (*DDX18*) and distally by the coiled-coil domain containing 93 gene (*CCDC93*). A predicted gene *XR_017010* is also localized in this region. Other likely candidate genes for this syndrome are localized further distal from the breakpoint (Figure 3). The first is the insulin-induced protein 2 (*INSIG2*) or the INSIG2 membrane protein, which is localized about 180 kb distal to the breakpoint region, whereas the second is the homeobox protein engrailed-1 (*EN1*), about 930 kb distal to the breakpoint.

Owing to the impossibility of obtaining an additional sample from this proband, mapping of the chromosome 4 breakpoint was not feasible. However, no obvious candidate gene was identified at the distal end of the long

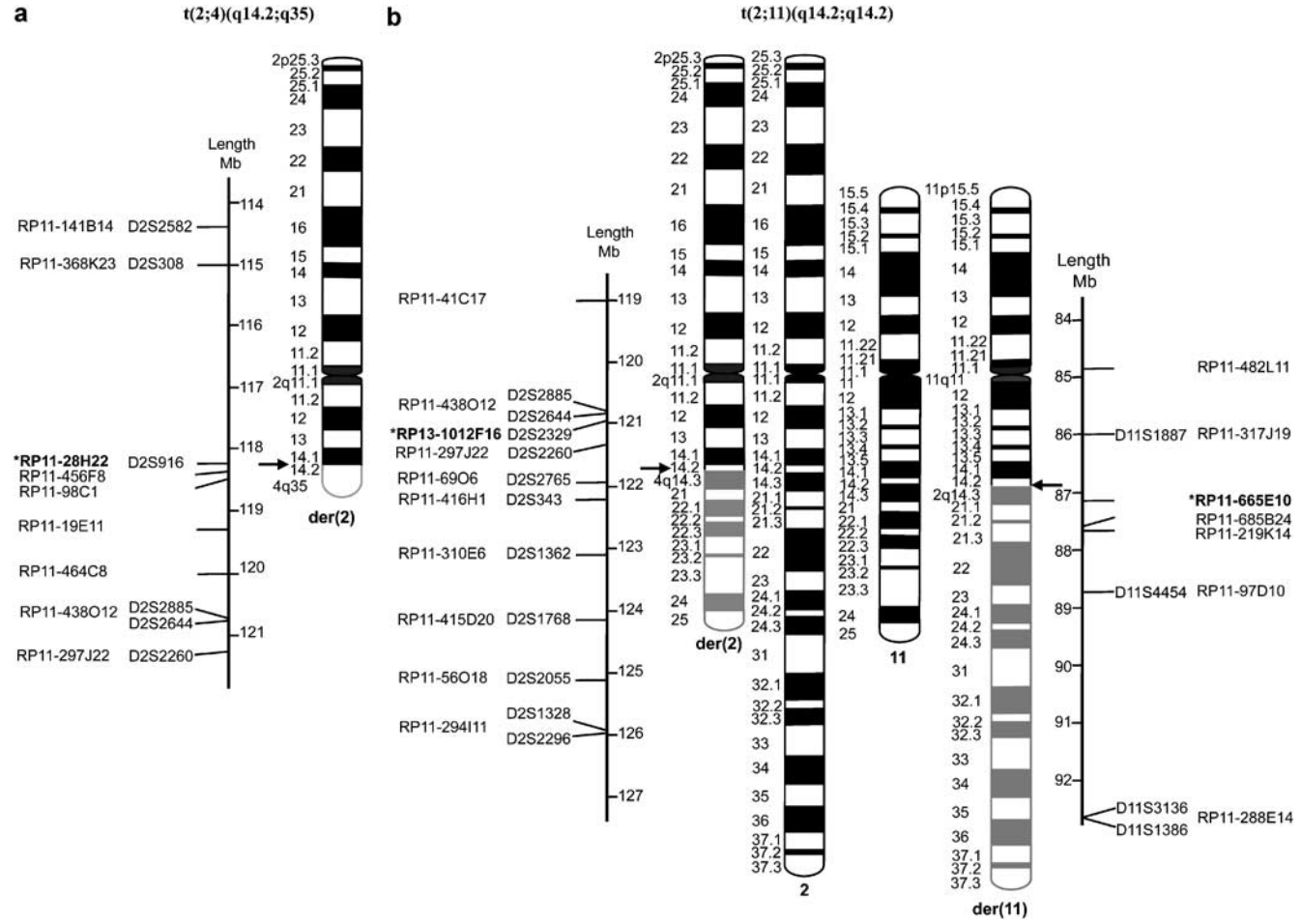

Figure 2 Mapping of the translocation breakpoints. Arrows indicate chromosome breakpoints. The physical map of the STS markers and corresponding BAC clones used for FISH analysis are indicated along the derivative chromosome ideograms. The breakpoint-spanning BAC clones are marked with an asterisk and are in bold. Distances between markers are according to the ensemble database. (**a**) Ideogram of the der(2) chromosome of the t(2;4)(q14.1;q35). (**b**) Ideograms showing the normal and derivative chromosomes from the [t(2,11)(q14.2;q14.2)] translocation.

arm of chromosome 4, in the cytogenetically established breakpoint region (q35.1–q35.2).

Mapping of the chromosome 11 breakpoint and candidate genes from this region

The chromosome 11 breakpoint spanning BAC clone RP11-665E10 (localized at 87 156–87 317 kb) was identified as described above (Figure 1e and 2b). This breakpoint is situated about 250 kb proximal of the RAS oncogene family member RAB38 gene (*RAB38*) in a gene-poor region (Supplementary Figure 1). Presently, none of the genes localized in this breakpoint region are considered as candidates for the SFM phenotype.

Screening of the *INHBB*, *GLI2*, *XR_017842*, *EN1* and *INSIG2* candidate genes

Several unreported alterations were identified in the 5′UTR of *INHBB*. The C>T alteration at position c.-167 was identified in several patients, with a frequency of the T allele of about 10%. This alteration creates a potential donor splice site with a consensus value (CV) of 0.70 *vs* 0.52, whereas the donor splice site CV of exon 1 is 0.86. A novel STR at position c.-103: $(CGGGCG)_{2-5,}$ flanked 5′ by $(CGGG)_4$ and 3′ by $(GGGGC)_3$, was also identified. The frequencies of the different alleles in the unrelated patients *vs* controls were: $(CGGGCG)_2$ 1.7 *vs* 1.7%, $(CGGGCG)_3$ 26 *vs* 22%, $(CGGGCG)_4$ 72 *vs* 74% and $(CGGGCG)_5$ 0 *vs* 1.7%. In the $(CGGG)_4$, repeat an additional polymorphic alteration c.-135G>A was also observed. Finally, at position c.-18, a C>G alteration was also identified in one patient.

In addition to the above reported alterations in the 5′UTR, two previously reported coding-region polymorphisms were also found: Ser47Ala (SNP ID rs11900747) in exon 1, and His208His (c.624T>C, SNP ID rs4328642) in exon 2 of *INHBB*. The frequency of the A47 variant was 6%, whereas that of the allele c.624T was 1.4% in the patient group. One patient (no. 16637) was identified with the following haplotypes: c.-167C/T, (CGGGCG)2/4, Ser47Ala.

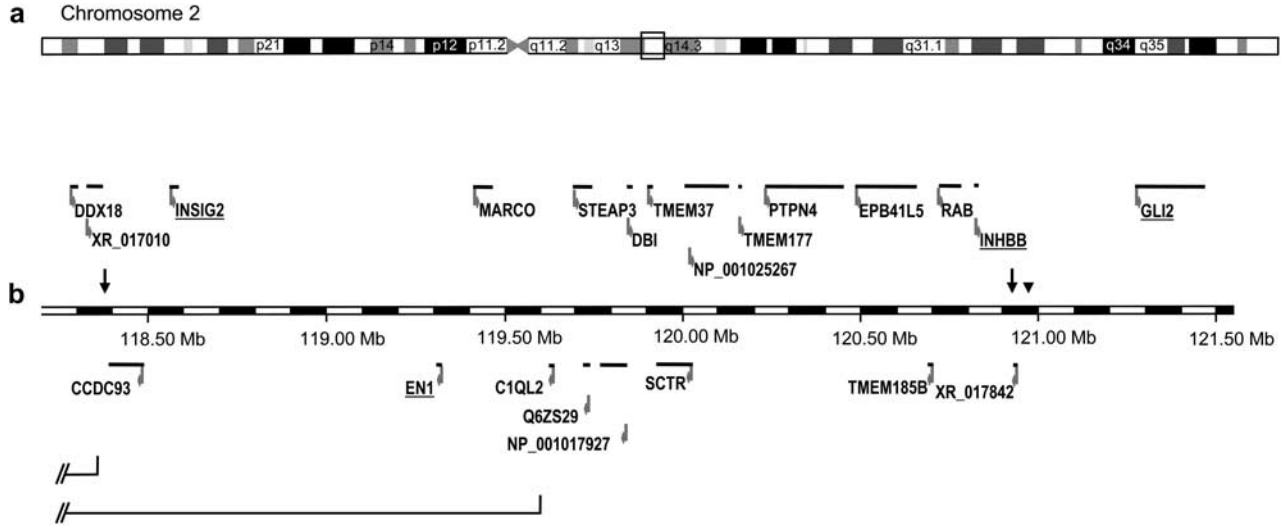

Figure 3 Comparative map of the two breakpoints on the long arm of chromosome 2. (**a**) Schematic ideogram of chromosome 2; the breakpoints region is highlighted by a box. (**b**) Detailed physical map across this region. Horizontal lines with arrowheads indicate the position of genes in sense (above the map) and antisense (below the map) orientation. The most important candidate genes are underlined. Arrows indicate the location of the breakpoints mapped in this study. The recently reported breakpoint associated with SHFLD is indicated by an arrowhead.[11] The distal ends of two deletions, a 4.5–6.0 Mb in 2q14.1 and a 2–3 Mb deletion in 2q14.2, reported by Barber *et al*[30] are also indicated.

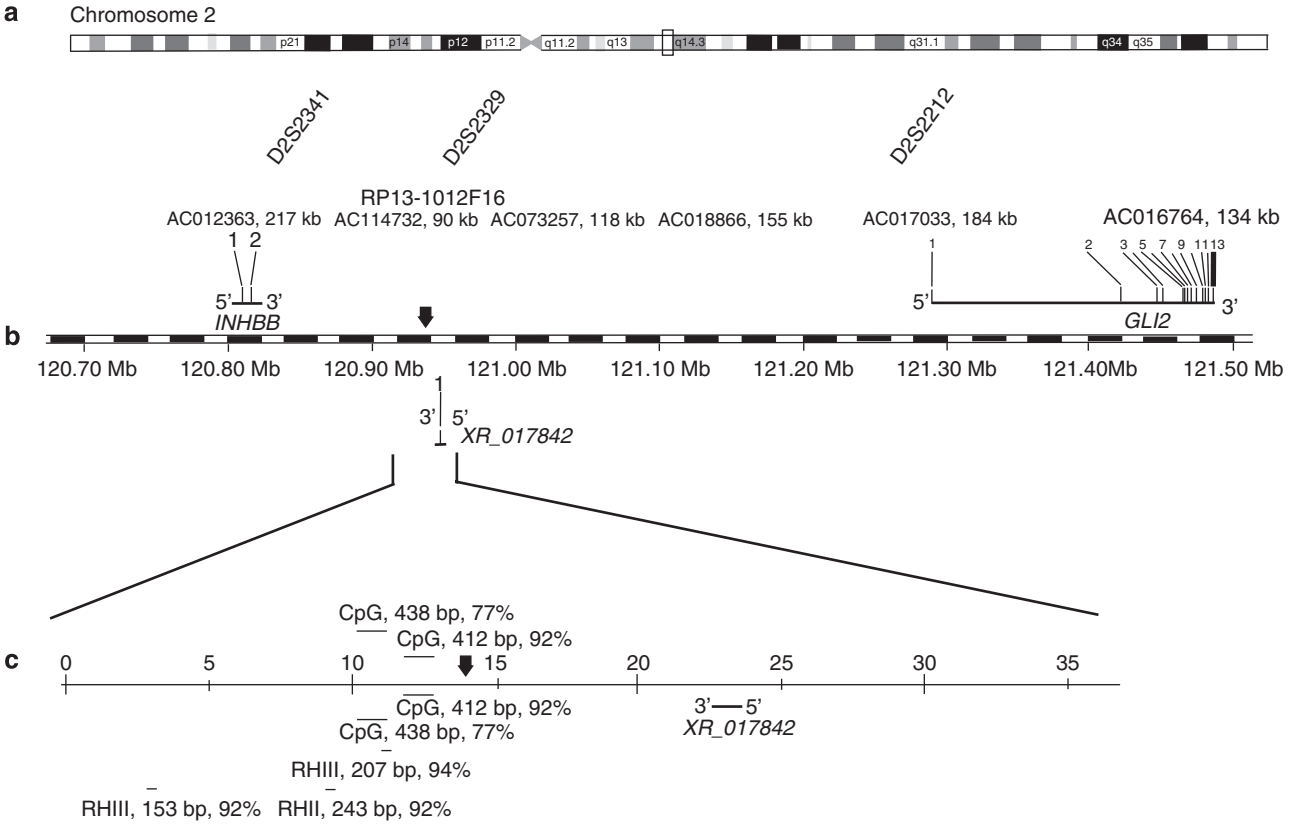

Figure 4 Schematic representation of the chromosome 2 breakpoint region associated with isolated SFM. (**a**) Schematic ideogram of chromosome 2; the breakpoint region is highlighted by a box. (**b**) Physical map across the chromosome 2 breakpoint region. Some of the STS markers from this region, together with the GeneBank sequence acc. no. of BACs spanning this region, are noted above the map. Location and genomic organization of the candidate genes are indicated. Numbered vertical lines indicate exons. (**c**) Detailed map of the breakpoint region indicating the position of evolutionarily conserved sequence elements and of CpG islands. Arrow indicates the location of the breakpoint.

Several reported or novel, most likely polymorphic, intronic alterations were also identified in the *GLI2*: IVS3-17G>T; IVS4+24G>A (SNP ID rs12614482) and IVS4+35C>T (SNP ID rs12617878); IVS6-26G>A and IVS6-28T>C (SNP ID rs2592591); and IVS10+49T>C (SNP ID rs280196).

Novel or already reported alterations were also identified in the coding regions of the *GLI2*: in exon 5 Ser267Ser (SNP ID rs2592595); in exon 11, an unreported c.1761G>T Thr587Thr and a reported Thr649Thr (SNP ID rs13008360) silent alteration; in exon 13 Ala1156Ser (SNP ID rs3738880), Asp1306Asn (SNP ID rs12711538), Pro1313Pro (SNP ID rs10167980), and c.3943, Pro1315Ser. The latest variant was reported as being likely polymorphic[16] and the allelic frequency of this was 0.069 in the patient group. This variant was also found in homozygosity in one patient.

Interestingly, in patient no.16706 a dinucleotide mutation c.4332_4333GC>AT, led to amino acid substitutions Met1444Ile and Leu1445Phe, whereas, in patient no.16928, double missense mutations, c.4558G>A, Asp1520Asn and c. 4054A>G, Met1352Val, were identified. Both are segregating in *cis* on the same alleles. These variants were screened in a control population; the frequency of the dinucleotide alteration was 0.003 in 330 unrelated chromosomes, whereas that of the Asn1520 - Val1352 variant was 0.012 (in 162 unrelated chromosomes). Screening of the parents of the proband with the Asn1520 - Val1352 variant revealed that this was inherited from his phenotypically normal mother.

Most of the patients were informative for several polymorphisms in these candidate genes, and therefore deletion of these can be excluded in the large majority of the proband.

In the third hypothetical gene, *XR_017842*, no alteration was found other then the previously reported Cys138Tyr polymorphism (SNP ID rs17050160). The frequency of the Tyr138 variant in the patient group was 0.095 *vs* 0.065 in the control group.

No DNA variants were detected in the *EN1* gene or in the three patients with SHFM and holoprosencephaly who were screened for mutation in the *INSIG2* gene.

QRT-PCR

SYBR green-based QRT-PCR analysis revealed that the expression level of *INHBB* and *GLI2* in eight control LCLs was barely detectable and too low to allow reliable quantification. In patient cells, the expression of both genes was low as well, but more readily detectable than in the control LCLs, indicating that, if anything, expression of these is increased rather than decreased.

Discussion

Comparative analysis of two 2q41.2 translocation breakpoints associated with ectrodactyly revealed, to our surprise, that these were separated by approximately 2.5 Mb of genomic sequence. The breakpoint associated with SFM was mapped to position 120 922 kb and colocalizes with a recently reported breakpoint associated with SHFLD.[11] The second breakpoint, associated with HHES, was mapped to position 118.4 Mb of chromosome 2, which is actually distal 2q41.1 and not 2q41.2. Several strong candidate genes were identified in these *loci*, including *GLI2*, *INHBB*, *INSIG2* and *EN1*, which can all be easily correlated with Sonic Hedgehog (SHH) signalling and the observed phenotypes. Failure to identify convincing matching gene mutations in these genes may reflect the specific disease mechanism that is brought about by the translocations. Furthermore, there is no evidence for reduced transcription of the candidate genes, *GLI2* and *INHBB*, in the LCL of the patient with SFM. It is plausible that the translocations disrupt the specific arrangement of long-range regulatory elements that control the tight quantitative spatiotemporal expression of one or more genes from the breakpoint region. Disruption of such long-range regulation mechanisms has been reported earlier for *SHH* and *GLI3*, notably also in disrupted limb development with or without holoprosencephaly (Kleinjan and van Heyningen,[17] and references therein). Below, we will discuss these aspects specifically.

Candidate genes at the breakpoint regions

Two translocation breakpoints, only 40 kb apart, colocalize in the intergenic region between *INHBB* and *GLI2*. GLI2 is a member of the family of GLI zinc-finger transcription factors that mediate SHH signalling. This family of genes (*GLI1*, *GLI2* and *GLI3*) plays an essential role in embryonic development and carcinogenesis. Members of this family have distinct as well as overlapping functions. GLI2 and GLI3 are the primary mediator transcription factors of the SHH signal. GLI3 acts mainly as a transcriptional repressor, whereas GLI2 is regarded primarily as an activator with weak repressor activity (reviewed by Koebernick and Pieler[18]). The SHH signal effector GLI2 has been implicated in a number of embryonic developmental processes and pathways. GLI2-deficient mice show multiple developmental defects in several organ systems including the skeleton of the limbs, and its presence is also necessary for normal endochondral development.[18,19] Recent data presented by Zhao *et al*[20] showed that Gli2, mediating the SHH signal, is a powerful activator of bone morphogenetic protein 2 (BMP2) expression, which also plays a critical role in osteoblast function and embryonic skeletal development. The graded morphogen SHH is expressed in the zone of polarizing activity (ZPA). The importance of SHH signalling, as well as of the Shh-regulated Gli3 for digit formation and limb skeletal patterning, is well known (reviewed by Nieuwenhuis and Hui[21]).

The second candidate gene from this region is *INHBB*. Activins/inhibins are members of the TGFß super-family.

INHBB is one of the activin/inhibin ß-subunits (ßA, ßB, ßC, ßE) that enter into the assembly of the activin/inhibin ligand dimers (reviewed by Thompson *et al*[22]).

Activins or inhibins are best known for their endocrine role in pituitary follicle-stimulating hormone synthesis and secretion and for their reproductive function. Besides these functions, Merino *et al*[23] very convincingly showed an important role of activin/inhibin signalling in digital skeletogenesis. They showed that exogenous implantation in the interdigital mesoderm of chick embryos of various dimers of activins leads to extra digit formation, whereas follistatin, a natural antagonist of these, blocks activin-induced or physiological digit formation. Furthermore, they also showed the interaction of activins with BMPs. Despite this, no major anomalies were observed in homozygous null mutant mice for activin-βB other than the failure of eyelid fusion.[24]

Comparative mapping of the HHES-associated chromosome 2 breakpoint localized it approximately 2.5 Mb proximal to the previous one. The *INSIG2* gene localizes approximately 150 kb distal to the breakpoint and encodes an endoplasmic reticulum anchor protein. Several lines of evidence indicate that *INSIG2* is a pivotal gene for regulation of lipid and cholesterol metabolism and a susceptibility gene for circulating levels of cholesterol.[25] In addition, INSIG2 acts as a key regulator of cholesterol synthesis by blocking the transport of sterol regulatory element-binding protein to the Golgi.[26]

An overlap of developmental malformations has been observed between defects of cholesterol biosynthesis and of SHH signal transduction, and indeed both have been associated with holoprosencephaly as well as limb malformations.[27] Although, simultaneously to the autoprocessing reaction of SHH, sterol modification is required for efficient signal biogenesis, the phenotypic overlap mentioned above can more likely be explained by a direct effect of sterol deprivation on Smoothened (Smo), a receptor-associated transmembrane protein, that is essential for SHH signal transduction.[27] Therefore, the disturbance of cholesterol homoeostasis owing to the altered expression of *INSIG2* may well represent a factor contributing to altered SHH signalling, leading to the reported HHES in the proband. The second candidate gene from this region is *EN1*, which is within the range of a possible position effect (1 Mb). EN1 is one of the human orthologs of the *Drosophila* engrailed homeodomain containing transcription factor. Several lines of evidence, mainly obtained through transgenic mouse studies, indicate that its main function is in the mid-hindbrain and limb development.[28,29] The limb phenotype designated as 'double dorsal' with structural anomalies such as truncations, fusions and supernumerary digits, as well as delay in its ossification, were described in these transgenics.[29] These anomalies reflect its role in dorsal–ventral axis patterning as well as in AER formation. In humans, haploinsufficiency of this gene does not necessarily lead to an abnormal phenotype.[30]

DNA alterations identified in the candidate genes

The identification of a pathogenic mutation within one of these candidate genes, in non-translocation patients presenting similar congenital anomalies, would unequivocally implicate this gene in the aetiology of the corresponding malformation. Several unreported mutations have been identified in introns or in UTRs of the candidate genes. All of these were evaluated as potential cryptic splice sites or branch point sites. Presently, on the basis of our current knowledge, none of these can be considered as a pathogenic mutation. Among the identified amino-acid substitutions, the most important is the double mutation (c.4558G>A, Asp1520Asn and c. 4054A>G, Met1352Val) in the *GLI2* gene of an isolated patient with nonsyndromic SHFM. The high level of conservation of residue Asp1520 (Supplementary Table) suggests that this double mutation may well be pathogenic, but surprisingly, this was also identified in the control group and was inherited from a phenotypically normal mother. Loss-of-function mutations in GLI2 have been associated with a phenotype of defective anterior pituitary formation, pan-hypopituitarism and holoprosencephaly-like mid-facial hypoplasia.[16]

The fact that no clear pathogenic mutation was identified in these groups of patients (present study and Babbs *et al*[11]) and that QRT-PCR did not show any evidence for downregulation of *INHBB* and *GLI2* may reflect that the molecular alterations introduced by the translocations may have very specific effects in terms of quantitative spatiotemporal expression of one or more genes from the breakpoint regions. It is very likely that such effects may not be mimicked by intragenic gene mutations.

Molecular mechanism

The finding of three ectrodactyly-related translocations in 2q41.1–q41.2, the lack of intragenic mutations and an increased expression of the *INHBB* and *GLI2* genes in LCLs of the fetus with SFM is suggestive of complex long-range regulatory mechanisms for developmental genes (Figure 3). Several examples of long-range gene regulation have been described, in which chromosomal translocations exert positional effects on distant genes.[17] One of the most elegant demonstrations of such regulatory element was reported by Lettice *et al*[31] who identified a conserved element within an intron of a gene (*LMBR1*) situated about 1 Mb distal to the target gene *SHH*. Mutations in this conserved element cause ectopic expression of Shh and postaxial polydactyly. Interestingly, the region proximal to the SHH gene on 7q36 harbours the *INSIG1* and *EN2* genes, the paralogs of *INSIG2* and *EN1*, which are located in the 2q41 breakpoint region proximal to GLI2. The two breakpoints in our study are separated by 2.5 Mb, which is considerably larger in size than the distance covered by any

long-range element described so far.[17] On the basis of the present data, we entertain two possible explanations for our results.

One possibility is that all breakpoints affect the developmental expression of one or more genes from this region by disruption of the architecture of their corresponding long-range control elements. In this scenario, long-range control elements must be operational at very long distances from the target site, given the large separation of the two translocation breakpoints. The alternative possibility is that positional effects introduced by the translocations lead to epigenetic alterations of the local chromatin structure, for example by inappropriate DNA methylation or histone modifications. Both possible mechanisms are predicted to result in quantitative spatiotemporal disrupted expression of one or several genes during embryonic development.

The very low expression levels of the candidate genes *INHBB* and *GLI2* in lymphoblast cell lines prohibited their quantitative analysis for their possible involvement. It is very likely that such studies can be reliably performed only by using material from tissues obtained from appropriate developmental stages. Therefore, further research should focus on the identification of long-range regulatory elements that control transcription of genes in the region encompassing the breakpoints. Such elements may be binding sites for transcription factors such as TP63, which is mutated in a number of syndromes that have SHFM as a major hallmark. Ultimately, the identification of specific functional mutations in such elements, such as microdeletions and nucleotide changes, in SHFM patients has to prove the functionality of such elements in health and disease.

Acknowledgements

We thank Purificação Tavares for pre-natal diagnosis of the translocation; Anabela L Dias for maintaining the LCL; Catarina Reis for contributing to the screening of the 5′UTR of INHBB*; Sara Malveiro for contributing to fine mapping of the chromosome 2 breakpoint; Emine Bolat for quantitative RT-PCR analysis; Paula Borralho and Ricardo Laurini, for morphopathological evaluation of the abortus; and Raoul Hennekam for contributing patient material. This project was partially supported by* Fundação para a Ciência e a Tecnologia *research Grant POCTI/MGI/38649/2001, by* Programa de Financiamento Plurianual do CIGMH *and by* Fundo Comunitário Europeu FEDER*, and the European Union Sixth Framework program EpiStem project (LSHB-CT-2005-019067).*

References

1 Duijf PHG, van Bokhoven H, Brunner HG: Pathogenesis of split-hand/split-foot malformation. *Hum Mol Genet* 2003; **12**: R51–R60.
2 Van Bokhoven H, Brunner HG: Splitting p63. *Am J Hum Genet* 2002; **71**: 1–13.
3 Kjaer KW, Hansen L, Schwabe GC *et al*: Distinct *CDH3* mutations cause ectodermal dysplasia, ectrodactyly, macular dystrophy (EEM syndrome). *J Med Genet* 2005; **42**: 292–298.
4 Bernardini L, Palka C, Ceccarini C *et al*: Complex rearrangement of chromosome 7q21.13-q22.1 confirms the ectrodactyly-deafness locus and suggests new candidate genes. *Am J Med Genet* 2008; **146A**: 238–244.
5 de Mollerat XJ, Gurrieri F, Morgan CT *et al*: A genomic rearrangement resulting in a tandem duplication is associated with split hand-split foot malformation 3 (SHFM3) at 10q24. *Hum Mol Genet* 2003; **12**: 1959–1971.
6 Goodman FR, Majewski F, Collins AL, Scambler PJ: A 117-kb microdeletion removing HOXD9-HOXD13 and EVX2 causes synpolydactyly. *Am J Hum Genet* 2002; **70**: 547–555.
7 Gurnett CA, Dobbs MB, Nordsieck EJ *et al*: Evidence for an additional locus for split hand/foot malformation in chromosome region 8q21.11-q22.3. *Am J Med Genet* 2006; **140A**: 1744–1748.
8 Corona-Rivera A, Corona-Rivera JR, Bobadilla-Morales L, García-Cobian TA, Corona-Rivera E: Holoprosencephaly, hypertelorism, and ectrodactyly in a boy with an apparently balanced *de novo* t(2;4) (q14.2;q35). *Am J Med Genet* 2000; **90**: 423–426.
9 König R, Beeg T, Tariverdian G, Scheffer H, Bitter K: Holoprosencephaly, bilateral cleft lip and palate and ectrodactyly: another case and follow up. *Clin Dysmorphol* 2003; **12**: 221–225.
10 Naveed M, Nath SK, Gaines M *et al*: Genomewide linkage scan for split-hand/foot malformation with long-bone deficiency in a large Arab family identifies two novel susceptibility loci on chromosomes 1q42.2-q43 and 6q14.1. *Am J Hum Genet* 2007; **80**: 105–111.
11 Babbs C, Heller R, Everman DB *et al*: A new locus for split hand/foot malformation with long bone deficiency (SHFLD) at 2q14.2 identified from a chromosome translocation. *Hum Genet* 2007; **122**: 191–199.
12 Van Roy N, Jauch A, Van Gele M *et al*: Comparative genomic hybridization analysis of human neuroblastomas: detection of distal lp deletions and further molecular genetic characterization of neuroblastoma cell lines. *Cancer Genet Cytogenet* 1997; **97**: 135–142.
13 David D, Cardoso J, Marques B *et al*: Molecular characterization of a familial translocation implicates disruption of HDAC9 and possible position effect on TGFbeta2 in the pathogenesis of Peters' anomaly. *Genomics* 2003; **81**: 489–503.
14 David D, Ribeiro S, Ferrão L, Gago T, Campos M, Crespo F: Molecular basis of inherited antithrombin deficiency in Portuguese families: identification of underlying molecular defects and screening for additional thrombotic risk factors. *Am J Hematol* 2004; **76**: 163–171.
15 de Brouwer AP, van Bokhoven H, Kremer H: Comparison of 12 reference genes for normalization of gene expression levels in Epstein-Barr virus-transformed lymphoblastoid cell lines and fibroblasts. *Mol Diagn Ther* 2006; **10**: 197–204.
16 Roessler E, Du YZ, Mullor JL *et al*: Loss-of-function mutations in the human GLI2 gene are associated with pituitary anomalies and holoprosencephaly-like features. *Proc Natl Acad Sci USA* 2003; **100**: 13424–13429.
17 Kleinjan DA, van Heyningen V: Long-range control of gene expression: emerging mechanisms and disruption in disease. *Am J Hum Genet* 2005; **76**: 8–32.
18 Koebernick K, Pieler T: Gli-type zinc finger proteins as bipotential transducers of Hedgehog signaling. *Differentiation* 2002; **70**: 69–76.
19 Miao D, Liu H, Plut P *et al*: Impaired endochondral bone development and osteopenia in Gli2-deficient mice. *Exp Cell Res* 2004; **294**: 210–222.
20 Zhao M, Qiao M, Harris SE, Chen D, Oyajobi BO, Mundy GR: The zinc finger transcription factor Gli2 mediates bone morpho-

genetic protein 2 expression in osteoblasts in response to hedgehog signaling. *Mol Cell Biol* 2006; **26**: 6197–6208.
21 Nieuwenhuis E, Hui C-C: Hedgehog signaling and congenital malformations. *Clin Genet* 2004; **67**: 193–208.
22 Thompson TB, Cook RW, Chapman SC, Jardetzky TS, Woodruff TK: Beta A versus beta B: is it merely a matter of expression? *Mol Cell Endocrinol* 2004; **225**: 9–17.
23 Merino R, Macias D, Gañan Y *et al*: Control of digit formation by activin signalling. *Development* 1999; **126**: 2161–2170.
24 Schrewe H, Gendron-Maguire M, Harbison ML, Gridley T: Mice homozygous for a null mutation of activin beta B are viable and fertile. *Mech Dev* 1994; **47**: 43–51.
25 Cervino AC, Li G, Edwards S *et al*: Integrating QTL and high-density SNP analyses in mice to identify Insig2 as a susceptibility gene for plasma cholesterol levels. *Genomics* 2005; **86**: 505–517.
26 Yabe D, Brown MS, Goldstein JL: Insig-2, a second endoplasmic reticulum protein that binds SCAP and blocks export of sterol regulatory element-binding proteins. *Proc Natl Acad Sci USA* 2002; **99**: 12753–12758.
27 Cooper MK, Wassif CA, Krakowiak PA *et al*: A defective response to Hedgehog signaling in disorders of cholesterol biosynthesis. *Nat Genet* 2003; **33**: 508–513.
28 Wurst W, Auerbach AB, Joyner AL: Multiple developmental defects in Engrailed-1 mutant mice: an early mid-hindbrain deletion and patterning defects in forelimbs and sternum. *Development* 1994; **120**: 2065–2075.
29 Loomis CA, Kimmel RA, Tong C-X, Michaud J, Joyner AL: Analysis of the genetic pathway leading to formation of ectopic apical ectodermal ridges in mouse Engrailed-1 mutant limbs. *Development* 1998; **125**: 1137–1148.
30 Barber JC, Maloney VK, Bewes B, Wakeling E: Deletions of 2q14 that include the homeobox engrailed 1 (EN1) transcription factor are compatible with a normal phenotype. *Eur J Hum Genet* 2006; **14**: 739–743.
31 Lettice LA, Heaney SJH, Purdie LA *et al*: A long-range Shh enhancer regulates expression in the developing limb and fin and is associated with preaxial polydactyly. *Hum Mol Genet* 2003; **12**: 1725–1735.

Supplementary Information accompanies the paper on European Journal of Human Genetics website (http://www.nature.com/ejhg)